Review

Progress in Hybrid Plasma Wakefield Acceleration

Bernhard Hidding, Ralph Assmann, Michael Bussmann, David Campbell, Yen-Yu Chang,
Sébastien Corde, Jurjen Couperus Cabadağ, Alexander Debus, Andreas Döpp, Max Gilljohann et al.

Special Issue

Review

Progress in Hybrid Plasma Wakefield Acceleration

Bernhard Hidding [1,2,*], Ralph Assmann [3,4], Michael Bussmann [5,6], David Campbell [1,2], Yen-Yu Chang [5], Sébastien Corde [7], Jurjen Couperus Cabadağ [5], Alexander Debus [5], Andreas Döpp [8], Max Gilljohann [7], J. Götzfried [8], F. Moritz Foerster [8], Florian Haberstroh [8], Fahim Habib [1,2], Thomas Heinemann [1,2], Dominik Hollatz [9,10], Arie Irman [5], Malte Kaluza [9,10], Stefan Karsch [8,11], Olena Kononenko [7], Alexander Knetsch [7], Thomas Kurz [5], Stephan Kuschel [12], Alexander Köhler [5], Alberto Martinez de la Ossa [3], Alastair Nutter [1,2,5], Richard Pausch [5], Gaurav Raj [7], Ulrich Schramm [5], Susanne Schöbel [5], Andreas Seidel [9,10], Klaus Steiniger [5], Patrick Ufer [5], Mark Yeung [9,10], Omid Zarini [5] and Matt Zepf [9,10]

1   Scottish Universities Physics Alliance SUPA, University of Strathclyde, 107 Rottenrow, Glasgow G4 0NG, UK
2   The Cockcroft Institute, Keckwick Ln, Daresbury, Warrington WA4 4AD, UK
3   Deutsches Elektronen-Synchrotron DESY, 22607 Hamburg, Germany
4   Laboratori Nazionali di Frascati, 00044 Frascati, Italy
5   Helmholtz-Zentrum Dresden-Rossendorf, Bautzner Landstraße 400, 01328 Dresden, Germany
6   Center for Advanced Systems Understanding CASUS, 02826 Görlitz, Germany
7   LOA, ENSTA Paris, CNRS, Ecole Polytechnique, Institut Polytechnique de Paris, 91762 Palaiseau, France
8   Faculty of Physics, Ludwig-Maximilians-Universität München, Am Coulombwall 1,
      85748 Garching, Germany
9   Institute of Optics and Quantum Electronics, Friedrich-Schiller-University of Jena, Max-Wien-Platz 1,
      07743 Jena, Germany
10   Helmholtz Institute Jena, Fröbelstieg 3, 07743 Jena, Germany
11   Max Planck Institut für Quantenoptik, Hans-Kopfermann-Straße 1, 85748 Garching, Germany
12   Center for Free Electron Science, CFEL, Luruper Chaussee 149, 22761 Hamburg, Germany
*   Correspondence: bernhard.hidding@strath.ac.uk

Abstract: Plasma wakefield accelerators can be driven either by intense laser pulses (LWFA) or by intense particle beams (PWFA). A third approach that combines the complementary advantages of both types of plasma wakefield accelerator has been established with increasing success over the last decade and is called hybrid LWFA→PWFA. Essentially, a compact LWFA is exploited to produce an energetic, high-current electron beam as a driver for a subsequent PWFA stage, which, in turn, is exploited for phase-constant, inherently laser-synchronized, quasi-static acceleration over extended acceleration lengths. The sum is greater than its parts: the approach not only provides a compact, cost-effective alternative to linac-driven PWFA for exploitation of PWFA and its advantages for acceleration and high-brightness beam generation, but extends the parameter range accessible for PWFA and, through the added benefit of co-location of inherently synchronized laser pulses, enables high-precision pump/probing, injection, seeding and unique experimental constellations, e.g., for beam coordination and collision experiments. We report on the accelerating progress of the approach achieved in a series of collaborative experiments and discuss future prospects and potential impact.

Keywords: plasma wakefield acceleration; LWFA; PWFA; compact particle acceleration; radiation sources

1. Introduction: LWFA and PWFA

The need for collective acceleration mechanisms as a pathway to overcome the limitations of conventional accelerators, such as the occurrence of voltage or structural breakdown, and to realize energy gains orders of magnitude larger than otherwise possible, has been discussed since the 1950s [1]. The electric fields in collective plasma electron oscillations increase with plasma density and were recognized to be suitable for achieving orders of magnitude larger energy gains. Using "lasers to accelerate electrons to high energies in a short distance" was proposed by Tajima and Dawson [2] in 1979 and is today

known as laser-driven plasma wakefield acceleration (LWFA). Using a "bunched relativistic electron beam in a cold plasma" was proposed by Chen et al. [3] in 1985 and is today known as particle beam-driven plasma wakefield acceleration (PWFA). Both schemes were visionary and required technological advances that were achieved over recent decades. For LWFA, a technological breakthrough came from the chirped pulse amplification (CPA) technique proposed by Strickland and Mourou [4] (interestingly, published in the same year as the seminal PWFA paper). CPA eventually made high-power, high intensity, ultra-short laser pulses commercially available, which, in turn, enabled the realization and exploitation of LWFA and the injection of electrons from background plasma wave-breaking and quasi-monoenergetic electron beam production [5] even in university-scale laboratories. For PWFA, the development was, perhaps, a little more gradual, with the first driver/witness-type double-bunch acceleration experiment performed in 1988 [6]. This was similar to the approach described in [3] as a driving/driven beam system, with two-bunch acceleration remaining a key strategy [7] as a result of the ability of linacs to provide such driver/witness beam systems.

2. Hybrid LWFA→PWFA

The LWFA and PWFA techniques have complementary advantages. Resulting from a strength and weakness analysis of both approaches, the concept of "hybrid laser-plasma accelerators" was established in 2010 [8]. The similarities, differences, and complementarities of LWFA and PWFA, and the resulting opportunities, are discussed in detail elsewhere, for example in [9–15]. As a top-level summary, the key complementary features are that laser pulses are ideal for tailored plasma production and use of LWFA for compact generation of intense, high-current electron beams, but suffer from dephasing, diffraction, and oscillatory electromagnetic field structures, whereas PWFA is ideal for dephasing-free, i.e., phase-constant and quasi-static acceleration over naturally long distances, operation in tailored pre-ionized plasma channels and ultracold electron beam production. Jointly, they provide inherent laser synchronization of systems to PWFA, for example, for probing, diagnostics and injection of high-brightness beams.

Figure 1 below illustrates the concept. In the LWFA stage, a laser pulse, with power of the order of 100 TW, propagates with a group velocity $v_g < c$ through plasma and drives a plasma wave with an elliptical "bubble" structure [16]. An electron beam is then injected by capturing plasma electrons in the accelerating longitudinal electric field, indicated by the blue profile. The electron beam is indicated in green and the transverse Lorentz-contracted fields are shown in red and blue, respectively. In the PWFA stage, this electron beam is used to drive the plasma wave in the "blowout" regime [17], with a velocity c without dephasing issues over long distances. A synchronized laser pulse(s) can then be used in arbitrary geometry for PWFA wakefield imaging or for advanced injection mechanisms and interaction experiments.
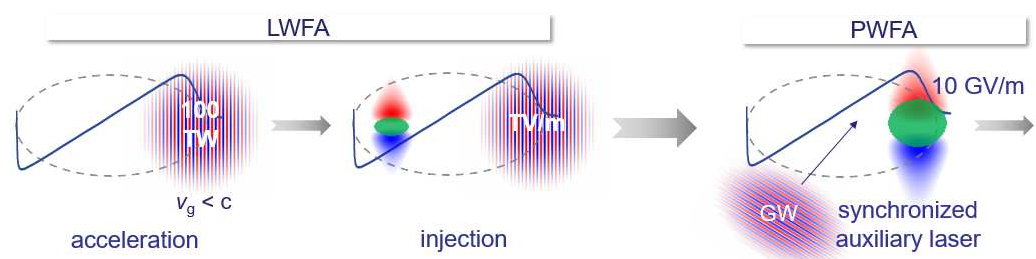
Figure 1. Schematic visualization of hybrid plasma wakefield acceleration. A 100 TW-scale laser pulse drives a wakefield (the blue line shows the profile of the longitudinal electric field on-axis); an electron beam is produced in the LWFA stage and then used as a driver for the attached PWFA stage. Here, the inherent advantages of PWFA for acceleration and injection and the inherent synchronization can be exploited.

Due to dephasing and laser depletion, a transition from laser-driven to electron-beam-driven regimes may occur quite naturally [18–24]. Figure 2a–c (adapted from [20]) shows how such a transition looks in PIC-simulations (also see Figure 8). Figure 2a depicts the plasma electron density distribution normalized by the critical density, which shows several electron bunches that have a pronounced effect on the wakefield structure. Figure 2b shows the corresponding transverse force normalized by $m_e c \omega$, and Figure 2c shows, in contrast to this, the transverse force that would be produced by the laser pulse only, without the electron bunch(es) present. Experimentally, this scenario manifests in enhanced betatron emission (length), in particular, for higher electron densities n_e, where dephasing and depletion are stronger (see Figure 2d).

While, in PWFA, laser pulses are not required, electron beams are always present in LWFA scenarios. Generally, the impact of injected electron beams is, therefore, inseparable from the LWFA process. For example, beam-loading [25] has been observed in seminal simulations that predicted mono-energetic electron bunch generation in LWFA [16], the increasing influence of the injected beam on the LWFA process was observed in simulations described in [18], beam-loading in LWFA experiments was observed in [26], and mode-transition from LWFA to PWFA [19] was encountered experimentally [21]. Such a gradual mode transition (also see Figure 8 and [15]) was suggested more recently to be responsible for energy spread improvement [24], while, conversely, it was interpreted, by the same group, for very similar beams from LWFA, that beam-driven acceleration was excluded [27] in experiments that provided highest-quality electron beams from LWFA that were used for the first demonstration of VUV-range free-electron lasing [28]. These examples underline the relevance of PWFA-like regimes for LWFA and show that both regimes may be more intertwined than is often appreciated. On the other hand, this also underlines the need for clear disentanglement between LWFA and PWFA stages and the need for 'safety margins' for purposeful, controlled injection processes, instead of sensitive at-threshold injection mechanisms and dark current production.

Reminiscent of the first driver/witness bunch pair experiments in linac-driven PWFAs, various mechanisms for the production of electron bunch trains from LWFA exist. The purposeful generation of electron bunch pairs from LWFA, for example, for driver/witness-type PWFA [7,8] was explored in [22] and measured via coherent transition radiation (CTR) of generated bunches. Figure 3 shows reconstructed electron bunch temporal profiles based on CTR signals for the cases of a short and long plasma cell, respectively. The longer plasma cell is longer than the dephasing distance, which implies a regime change from LWFA to PWFA, provided that the electron beam is strong enough when compared to the remaining laser pulse, and the injection of an additional electron bunch.

Informed by general studies of PWFA physics and enhanced energy gains, the staged combination of LWFA and PWFA become increasingly attractive as a result of the invention of the plasma photocathode, an injection scheme for generation of beams with orders of magnitude better emittance and brightness than state-of-the-art approaches. The plasma photocathode can act as a beam brightness transformer [29], in which the generated electron witness beam has much higher brightness than the incoming electron driver beam. While, for the first time, a plasma photocathode was developed with linac-driven PWFA [30], the inherent synchronization of plasma photocathode injection lasers with electron beams from LWFA, using a split-off laser pulse [31], makes this injection scheme ideally suited for hybrid LWFA→PWFA.

Plasma-lensing, a concept introduced in the context of high-energy physics [32], whereby plasma ions provide a focusing force [33], represents one of the initial stages in the quest to develop hybrid LWFA→PWFA. Figure 4 shows a setup used as a first step towards the development of staged hybrid plasma wakefield accelerators involving the use of two separated gas targets [34]. Here, the second gas target is pre-ionized by the diffracting LWFA remnant laser pulse and produces a plasma just ahead of the electron beam. The electron beam then undergoes plasma-lensing, which has a variety of applications, including capture of diverging electron beams from LWFA or transverse-

matching. While, in this setup, the laser pulse diffracted sufficiently and did not drive a plasma wave in the second gas jet, in a complementary setup produced earlier the laser pulse still drove a wakefield in the second jet and generated a focusing laser-driven plasma lens effect [35].
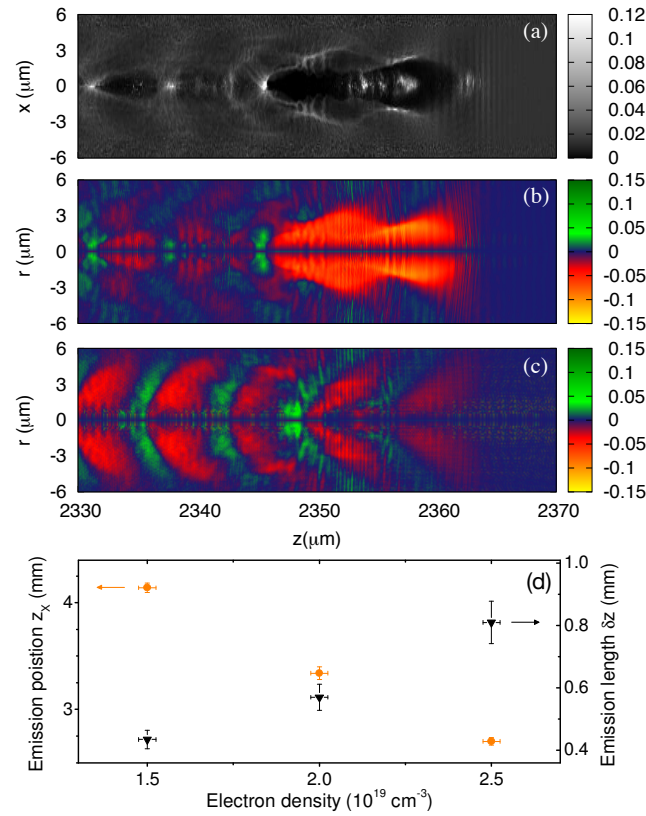

Figure 2. Mode transition: (**a**–**c**) show a PIC simulation at plasma density of $2.5 \times 10^{19} \, \text{cm}^{-3}$, in (**a**) plasma density n_e with the injected electron beam, in (**b**) the corresponding normalized transverse force in the wakefield and in (**c**) the transverse wakefield force as generated from the laser pulse only. This shows that, at this point, the wakefield is maintained primarily by the electron beam. In (**d**), experimental results showing that the betatron emission length and, thus, the plasma interaction length is increased with n_e at high values of n_e, contrary to LWFA scalings and in agreement with an LWFA-PWFA transition that allows for increased emission length at high plasma density (figure adapted from [20]).
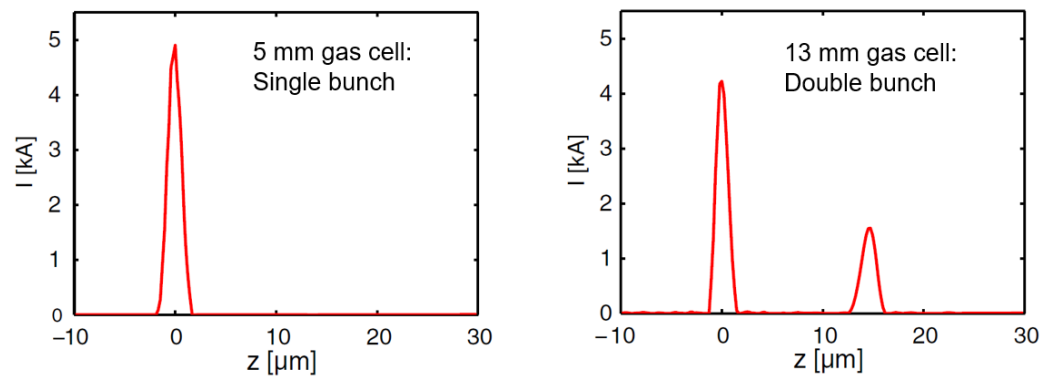

Figure 3. Single and double electron bunches produced from LWFA due to dephasing and a regime change from LWFA to PWFA, measured via coherent transition radiation (figure adapted from [22]).
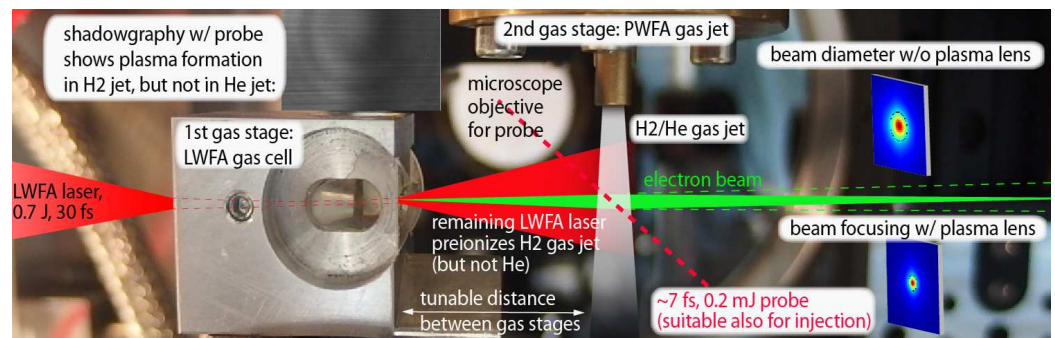
Figure 4. Hybrid setup with two separate gas targets used to show plasma-lensing of an electron beam in a second gas jet (figure adapted from [34]).

The next level of interaction intensity is reached when the electron beam from the LWFA stage has sufficient charge density and current that it begins to drive a plasma wave in the PWFA stage and, thereby, decelerates. Figure 5 shows the degree of deceleration observed when the second stage is placed at variable distances from the LWFA stage. Larger deceleration and, perhaps, some re-acceleration of decelerated electrons is obtained when the distance between both stages is shorter, consistent with the higher electron beam density and, hence, stronger wake driven by the diverging electron beam when the distance between the stages is reduced. Additionally, a steel tape was introduced in between the stages to rule out the potential for the LWFA laser remnant to interact with the PWFA stage. In this variation, the PWFA stage was self-ionized by the electric field of the electron beam—an important milestone in its own right and an indication of the high charge densities of electron beams obtainable from LWFA—and collective deceleration was observed [36].
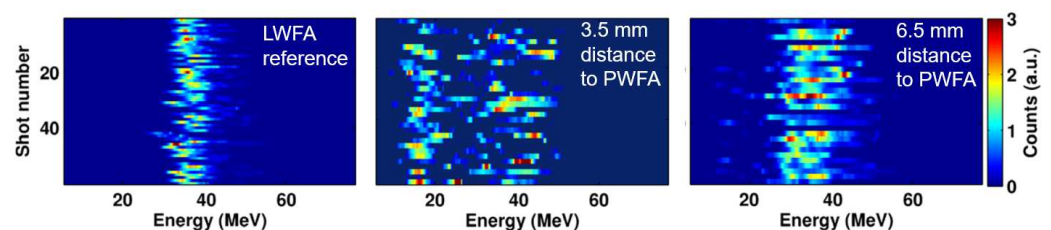

Figure 5. Collective deceleration shown using two separate targets, with varied distance of the PWFA to the LWFA jet (figure adapted from [36]).

The prospects of hybrid plasma wakefield accelerators, for example, as energy and brightness transformers, as PWFA physics test-beds, and to boost the capacities and capabilities of plasma wakefield accelerators, has increasingly fostered collaborative R&D in the US [29] and, in particular, in Europe [37], where, from 2017, a dedicated experimental collaboration, involving teams from Germany, France and the UK, was set up to systematically progress their development.

A first milestone of this collaboration was a demonstration that the capabilities of hybrid LWFA→PWFA can complement, and even exceed, those of linac-driven PWFA. In [11], a two-stage setup with a tape drive separation option was amended by a pre-ionizer laser pulse. The ultra-high electron beam density, which is obtained quite naturally from the LWFA stages, allowed driving of a plasma wave at densities of about $10^{19}\,\mathrm{cm}^{-3}$, about two orders of magnitude higher than those achieved in experiments conducted in the blowout regime at linac-driven PWFA facilities to date [7].

The inherent synchronization between electron beams and lasers was exploited for high-precision imaging of the dynamics at the PWFA stage via few-cycle shadowgraphy as used in LWFA [38]. Figure 6 shows that the strong, uni-polar electric field of the electron beam generates significant ion motion and an emerging cone structure. Time-resolved few-cycle shadowgrams of these dynamics are a powerful tool for PWFA research and

optimization in general. For example, it was concluded in [11] that this type of directed ion motion may have immediate implications for low-density PWFA as used at linac-based facilities. Specifically, it was highlighted that bunch trains, where the plasma might not be able to recover from the perturbation between two shots, should be investigated, a scenario that was later confirmed in [39]. These results show that time-resolved shadowgraphy, a technique that is standard in LWFA and was here introduced to (hybrid) PWFA, can provide fundamental insights, for example, into the dissipation of plasma waves [40] and energy transfer mechanisms [41] in PWFA.
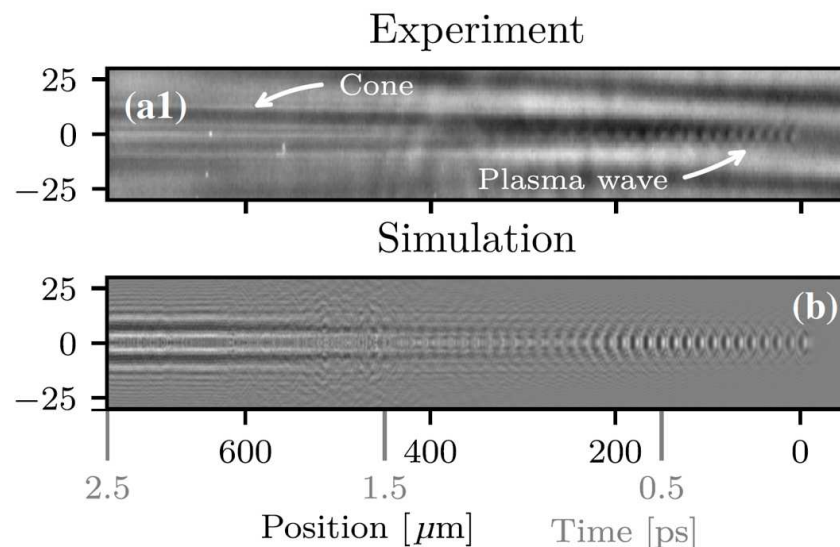
Figure 6. Experimentally imaged plasma wave obtained by shadowgraphy (**a1**) and corresponding simulation (**b**), illuminating the induced cone-shaped ion motion evolution as a result of the unipolar field kick of the PWFA (figure adapted from [11]).

The interaction of electron beams from LWFA with thin foils can involve filamentation in addition to emittance-spoiling scattering and is relevant for tape drive laser blockers between LWFA and PWFA stages, but also for staged LWFA schemes, where tape drives are used as plasma mirrors [42]. Figure 7 illustrates the effect of the laser-driven plasma instability in the foil on the LWFA electron beam, which was investigated in [43]. This research also demonstrated that the inherent synchronization between wakefield-accelerated electrons and laser pulses is very valuable for the probing and investigation of laser-plasma driven instabilities.

In [23], it was pointed out that electron beam quality optimization in LWFA is generally connected with operation at low charges (the same can be said about linacs, albeit for different reasons), while high charge beams are also required for many other applications than hybrid LWFA→PWFA. Ionization injection in LWFA [44] is naturally associated with high injection rates and, therefore, is a promising candidate for the production of heavily charged electron beams and exploitation of associated beam-loading [23]. Self-truncated ionization injection [45] has been realized as a localized, beam-loaded injection scheme with beam charges of hundreds of pC and currents of tens of kA [46], which are excellent prerequisites for laboratory-sized beam-driven plasma wakefield acceleration. Other schemes with high injection rates, such as density downramp injection, are also excellent approaches for the generation of high-current electron beams for PWFA.
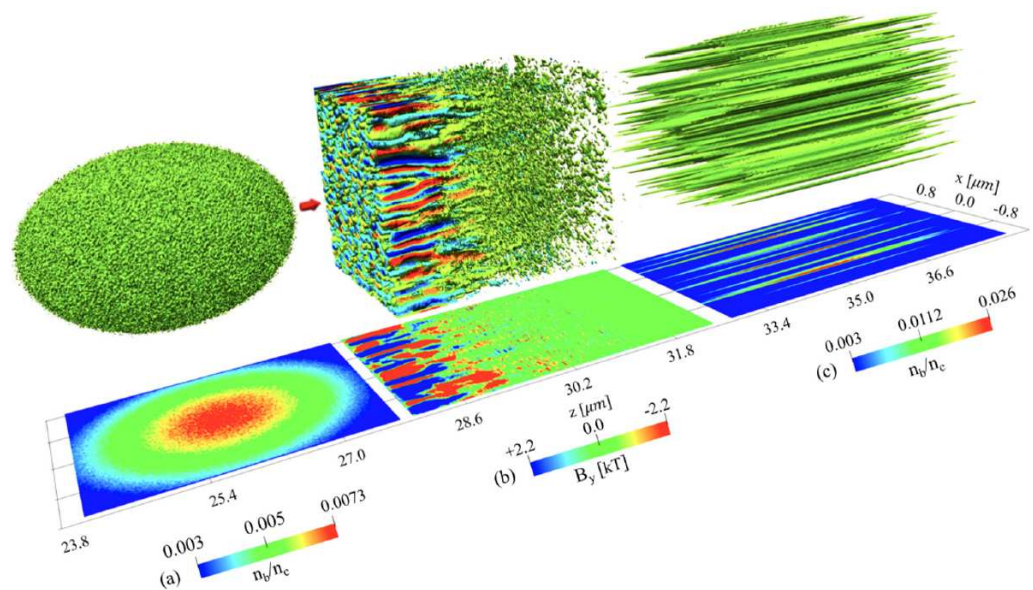
Figure 7. Laser-driven plasma instability probed by an electron beam from LWFA as a result of interaction between the laser pulse and the foil used as a laser blocker for separation of targets in LWFA→PWFA setups (figure adapted from [43]).

The physics of the transition from LWFA to PWFA, and the role of increasingly high charge, was further investigated in [15]. Figure 8 shows the different regimes and the transition from LWFA to PWFA when the laser pulse intensity and the electron beam charge, respectively, change. A pure unloaded LWFA regime is realized only when there is no injected electron beam, whereas, in contrast, a pure PWFA regime is realized only when the laser pulse vanishes. Different laser systems with different pulse durations and power levels, and two injection schemes for the LWFA stage, namely shock-front induced density downramp injection and colliding pulse injection, were used. By scanning across energies and plasma densities in the different regimes and setups, a wide range of scenarios, such as beam-loaded LWFA and beam-dominated wakefield scenarios, were experimentally realized. This included controlled production of two electron beams, which, in the context of hybrid LWFA→PWFA, are important for driver-witness-type acceleration [8] and the escort-beam loading approach for extremely high 6D-brightness beams [47].
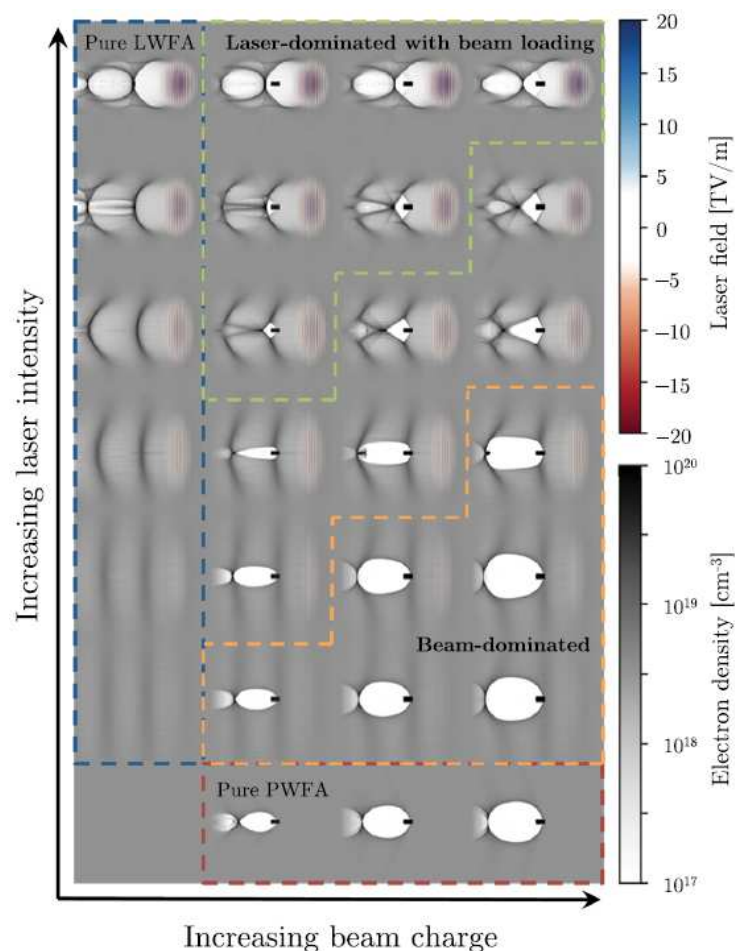
Figure 8. Overview showing a classification of laser pulse vs. electron-beam-dominated wakefield regimes (figure adapted from [15]). The electron beam charge density (*x*-axis) and the laser pulse intensity (*y*-axis) are responsible for the wake excitation and are, hence, decisive for the type of plasma wakefield that is generated.

3. Full Demonstration of Hybrid LWFA→PWFA

A breakthrough milestone was then passed that firmly established the LWFA→PWFA approach as an experimentally viable approach and platform. In [48], it was shown, for the first time, that driver/witness-type PWFA can be realized from an all-optical, laser-powered plasma wakefield accelerator. In Figure 9, the interaction setup is illustrated, along with plasma wave images of the LWFA stage, as well as the PWFA stage, in self-ionized and pre-ionized modes, respectively. The driver/witness pairs were generated via various mechanisms in the LWFA stage, separation between the two stages was realized with or without a tape drive laser blocker, and the platform was realized at two different laboratories. These results, with the feasibility as well as the variability demonstrated, and the similarity of the setups to the way they were envisioned a decade earlier [8], is a testament to the robustness and success of the approach, but also to its unique capabilities.

The inherently short duration and high charge density of electron beams from LWFA enable operation of the PWFA stage at naturally high plasma densities. The demonstrated energy gain gradient [48] of witness beams obtained in this first full-scale realization of LWFA→PWFA amounted to over 100 GeV/m, a rate similar to the highest ever achieved in linac-driven PWFA [49]. With regard to diagnostics, it is appropriate to emphasize again that the naturally synchronized interplay of up to three laser arms in these experiments [11,48], including a few-cycle optical probe beam, allows time-resolved shadowgraphy and, hence, illumination of the interaction with femtosecond resolution.

This capability is crucial for precision studies of plasma waves and dynamics and is also enormously useful for injection studies.
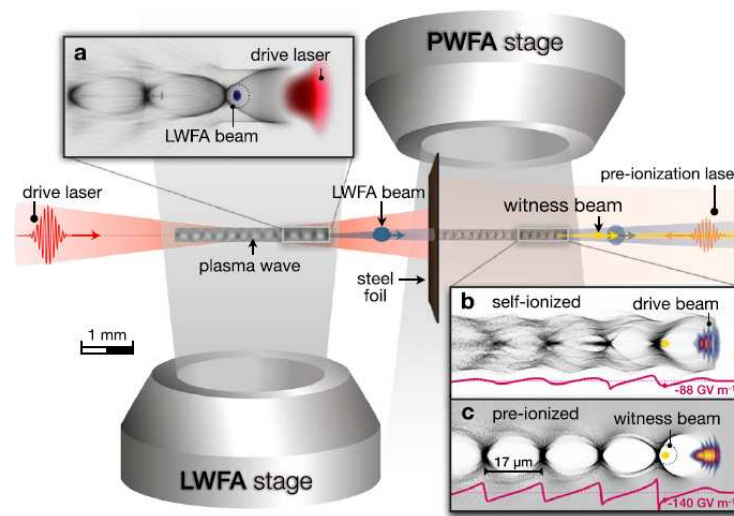

Figure 9. Hybrid LWFA→PWFA platform and driver/witness-type PWFA, using two separate gas jets and three laser arms to drive the LWFA stage and pre-ionize the PWFA stage for shadowgraphy imaging (figure adapted from [48]). The insets show simulation representations of LWFA and self-ionized and pre-ionized PWFA, respectively.

Gas-dynamic density downramp injection also represents a promising scheme for the production of high-quality electron beams. While a standard method in LWFA for more than a decade, its realization remained a long-harboured aspiration of the PWFA community until recently. Based on the now-established hybrid LWFA→PWFA platform [48], this milestone was reached in a straightforward manner. In [50], a thin wire was used to generate a (double) shock in the PWFA gas jet, with an associated downramp that captured plasma electrons and accelerated them at gradients beyond 120 GeV/m. Figure 10 shows the wire-equipped hybrid platform and the resulting hydrodynamic shock and gas density spike. The shadowgraphy was exploited to provide images of the shock(s) as well as the PWFA. Control of the injection parameters and the resulting electron beams was also demonstrated by changing the injection position as well as the plateau PWFA gas density. These results underline the rapid advance of the approach and the contributions it can make, for example, towards high-brightness electron beam generation.

The LWFA optimization priorities for electron beam generation for PWFA, such as charge and current, are different from those for traditional LWFA, where energy spread minimization is a key goal. While LWFA does not yet produce electron beams that can compete with state-of-the-art linacs in terms of stability, the variability can be exploited for passive parameter scans. In [51], an approximately inverse correlation between electron beam charge and energy [15] obtained in the LWFA due to beam loading was investigated through its impact on the PWFA stage. Jointly with PWFA shadowgraphy and other diagnostics, this allowed precision studies of the PWFA wakes to be carried through in the self-ionized and pre-ionized regimes, respectively. Relativistic plasma wave elongation, as a result of increased driver beam charge and density, was observed and, by probing the wake at different positions within the PWFA stage, the evolution of the decelerating driver beam and its corresponding plasma wake were observed. This setup will enable further in-depth studies of PWFA dynamics in the future.

In a recent study [52], for the first time, an all-optical injection scheme in hybrid LWFA→PWFA was realized. Here, an optically triggered shock provided the downramp; the approach thus complemented a first realization of the plasma photocathode [30] and plasma torch [53,54] methods, which had been first realized in linac-driven PWFAs. Moreover, Ref. [52] provided the first evidence that various aspects of stability, quality and

energy transfer of the generated electron beam obtained from injection in the PWFA stage can be improved. This represents a first step towards a beam brightness transformer based on the hybrid LWFA→PWFA platform.
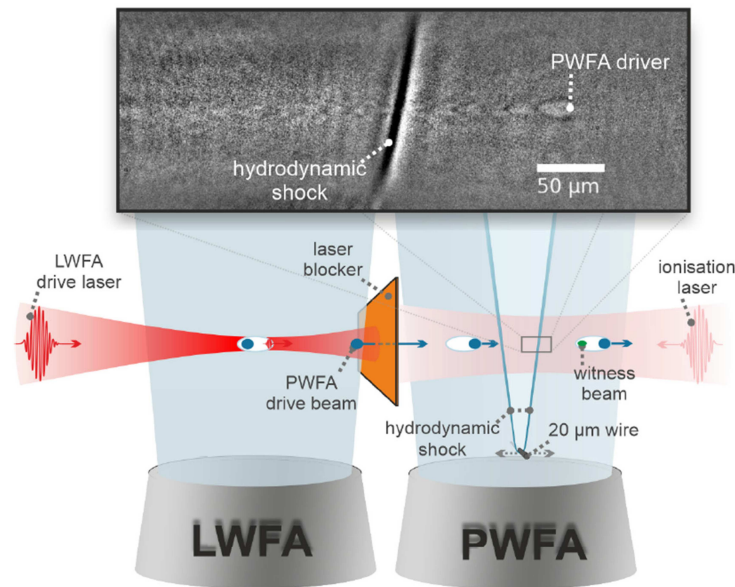

Figure 10. Gas-dynamic density downramp injection, realized by wire-induced shocks in the PWFA gas jet. Shadowgraphy reveals both the PWFA-driven plasma wave and the hydrodynamic shock profile (figure from [50]).

4. Conclusions

Both LWFA and PWFA, invented in their modern forms approximately four decades ago, have matured to become experimentally highly successful approaches. Each has particular advantages. Hybrid plasma wakefield acceleration, or LWFA→PWFA, seeks to exploit the best of both worlds and has been driven forward from innovation to realization with an increasing success rate over the last decade. This is not only because of the viability of the approach, but is also because of its capacities—there are only a small number of linac-driven PWFA facilities in the world, with corresponding limitations of access and accessible parameter ranges, constituting an R&D-capacity bottleneck. LWFA-driven PWFA systems, in contrast, can be realized in university-scale laboratories and, hence, offer a means of overcoming the capacity bottleneck that currently exists in PWFA. Moreover, LWFA→PWFA has already demonstrated capabilities beyond those of existing linac-driven PWFAs that can be exploited.

Figure 11 shows a timeline with experimental milestones passed over the last years as summarized in this paper.
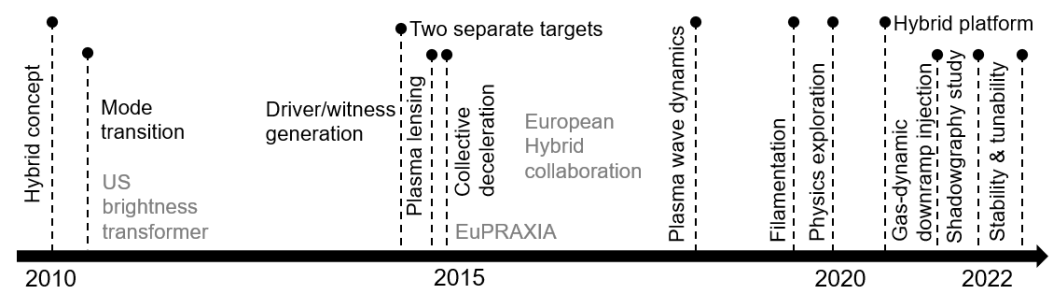
Figure 11. Timeline of hybrid LWFA→PWFA research, with selected experimental highlights. Milestones for the approach are being reached at an increasing rate based on the full experimental establishment of the hybrid plasma accelerator platform at the beginning of the 2020s.

What is next for LWFA→PWFA? One key prospect and goal is improvement in the quality of beams generated from these systems. In particular, plasma photocathodes provide promising quality boosts of several orders of magnitude, beyond even the highest-quality linac-generated electron beams and, at the same time, benefit from the inherent synchronization between electron beams and laser pulses in LWFA→PWFA. If such beam brightness transformers for laser-plasma accelerators can be realized, then this will have a transformative impact for various applications. These may include, light sources profitting from enhanced electron beam (phase space) density and brightness, creating prospects for X-ray free-electron-lasers [31,55,56], betatron radiation-based sources in X-ray and γ-ray [57] or ion channel laser regimes [55], or inverse-Compton-scattering-based γ-ray sources [9,55] driven by hybrid LWFA→PWFA. First experimental indications of free-electron-lasing in the VUV obtained from electron beams by LWFA [28] and in the IR from PWFA [58] via SASE, and as a seeded free-electron laser in the UV [59] from LWFA, have now been obtained. Start-to-end simulations show that, with high-brightness beams from plasma photocathodes, even attosecond-Angstrom-class hard X-FEL may become possible based on hybrid LWFA→PWFA systems [60]. Ultra-low emittance/ultra-high brightness beams are also of significant interest for high-energy physics research, for example, as test beams for staging and emittance preservation, and, in combination with co-located photon beams, also for, for example, nuclear- and quantum-electrodynamics research. We anticipate that, especially if the efforts that have been initiated for ultrabright electron beam production are successful with linac-driven PWFA and/or hybrid LWFA→PWFA, there will be a surge in laboratories engaging in hybrid LWFA→PWFA research as a gateway, not only to PWFA physics exploration, but also to ultrabright beam production and the myriad of resulting applications for next-generation experiments and science.

Data Availability Statement: Not applicable.

Conflicts of Interest: The authors declare no conflict of interest.

References

1. Lawson, J. Collective and coherent methods of particle acceleration. *Part. Accel.* **1972**, *3*, 21–33.
2. Tajima, T.; Dawson, J.M. Laser Electron-Accelerator. *Phys. Rev. Lett.* **1979**, *43*, 267–270. [CrossRef]
3. Chen, P.; Dawson, J.M.; Huff, R.W.; Katsouleas, T. Acceleration of Electrons by the Interaction of a Bunched Electron Beam with a Plasma. *Phys. Rev. Lett.* **1985**, *54*, 693–696. [CrossRef]
4. Strickland, D.; Mourou, G. Compression of amplified chirped optical pulses. *Opt. Commun.* **1985**, *56*, 219–221. [CrossRef]
5. Malka, V.; Faure, J.; Gauduel, Y.A.; Lefebvre, E.; Rousse, A.; Phuoc, K.T. Principles and applications of compact laser-plasma accelerators. *Nat. Phys.* **2008**, *4*, 447–453. [CrossRef]
6. Rosenzweig, J.B. Nonlinear plasma dynamics in the plasma wake-field accelerator. *Phys. Rev. Lett.* **1987**, *58*, 555–558. [CrossRef] [PubMed]
7. Litos, M.; Adli, E.; An, W.; Clarke, C.I.; Clayton, C.E.; Corde, S.; Delahaye, J.P.; England, R.J.; Fisher, A.S.; Frederico, J.; et al. High-efficiency acceleration of an electron beam in a plasma wakefield accelerator. *Nature* **2014**, *515*, 92–95. [CrossRef] [PubMed]
8. Hidding, B.; Koenigstein, T.; Osterholz, J.; Karsch, S.; Willi, O.; Pretzler, G. Monoenergetic Energy Doubling in a Hybrid Laser-Plasma Wakefield Accelerator. *Phys. Rev. Lett.* **2010**, *104*, 195002. [CrossRef]
9. Hidding, B.; Manahan, G.G.; Karger, O.; Knetsch, A.; Wittig, G.; Jaroszynski, D.A.; Sheng, Z.M.; Xi, Y.; Deng, A.; Rosenzweig, J.B.; et al. Ultrahigh brightness bunches from hybrid plasma accelerators as drivers of 5th generation light sources. *J. Phys. B At. Mol. Opt. Phys.* **2014**, *47*, 234010. [CrossRef]
10. Hidding, B.; Beaton, A.; Boulton, L.; Corde, S.; Doepp, A.; Habib, F.A.; Heinemann, T.; Irman, A.; Karsch, S.; Kirwan, G.; et al. Fundamentals and Applications of Hybrid LWFA-PWFA. *Appl. Sci.* **2019**, *9*, 2626. [CrossRef]
11. Gilljohann, M.F.; Ding, H.; Döpp, A.; Götzfried, J.; Schindler, S.; Schilling, G.; Corde, S.; Debus, A.; Heinemann, T.; Hidding, B.; et al. Direct Observation of Plasma Waves and Dynamics Induced by Laser-Accelerated Electron Beams. *Phys. Rev. X* **2019**, *9*, 011046. [CrossRef]
12. Hidding, B.; Foster, B.; Hogan, M.J.; Muggli, P.; Rosenzweig, J.B. Directions in plasma wakefield acceleration. *Philos. Trans. R. Soc. A Math. Phys. Eng. Sci.* **2019**, *377*, 20190215.
13. Martinez de la Ossa, A.; Assmann, R.W.; Bussmann, M.; Corde, S.; Cabadağ, J.P.C.; Debus, A.; Döpp, A.; Pousa, A.F.; Gilljohann, M.F.; Heinemann, T.; et al. Hybrid LWFA-PWFA staging as a beam energy and brightness transformer: conceptual design and simulations. *Philos. Trans. R. Soc. A Math. Phys. Eng. Sci.* **2019**, *377*, 20180175.
14. Manahan, G.G.; Habib, A.F.; Scherkl, P.; Ullmann, D.; Beaton, A.; Sutherland, A.; Kirwan, G.; Delinikolas, P.; Heinemann, T.; Altuijri, R.; et al. Advanced schemes for underdense plasma photocathode wakefield accelerators: Pathways towards ultrahigh brightness electron beams. *Philos. Trans. R. Soc. A Math. Phys. Eng. Sci.* **2019**, *377*, 20180182.
15. Götzfried, J.; Döpp, A.; Gilljohann, M.F.; Foerster, F.M.; Ding, H.; Schindler, S.; Schilling, G.; Buck, A.; Veisz, L.; Karsch, S. Physics of High-Charge Electron Beams in Laser-Plasma Wakefields. *Phys. Rev. X* **2020**, *10*, 041015. [CrossRef]
16. Pukhov, A.; Meyer-ter Vehn, J. Laser wake field acceleration: The highly non-linear broken-wave regime. *Appl. Phys. B-Lasers Opt.* **2002**, *74*, 355–361. [CrossRef]
17. Rosenzweig, J.B.; Breizman, B.; Katsouleas, T.; Su, J.J. Acceleration and focusing of electrons in two-dimensional nonlinear plasma wake fields. *Phys. Rev. A* **1991**, *44*, R6189–R6192. [CrossRef]
18. Tsung, F.S.; Narang, R.; Mori, W.B.; Joshi, C.; Fonseca, R.A.; Silva, L.O. Near-GeV-Energy Laser-Wakefield Acceleration of Self-Injected Electrons in a Centimeter-Scale Plasma Channel. *Phys. Rev. Lett.* **2004**, *93*, 185002. [CrossRef] [PubMed]
19. Pae, K.H.; Choi, I.W.; Lee, J. Self-mode-transition from laser wakefield accelerator to plasma wakefield accelerator of laser-driven plasma-based electron acceleration. *Phys. Plasmas* **2010**, *17*, 123104. [CrossRef]
20. Corde, S.; Thaury, C.; Phuoc, K.T.; Lifschitz, A.; Lambert, G.; Faure, J.; Lundh, O.; Benveniste, E.; Ben-Ismail, A.; Arantchuk, L.; et al. Mapping the X-ray Emission Region in a Laser-Plasma Accelerator. *Phys. Rev. Lett.* **2011**, *107*, 215004. [CrossRef] [PubMed]
21. Masson-Laborde, P.E.; Mo, M.Z.; Ali, A.; Fourmaux, S.; Lassonde, P.; Kieffer, J.C.; Rozmus, W.; Teychenné, D.; Fedosejevs, R. Giga-electronvolt electrons due to a transition from laser wakefield acceleration to plasma wakefield acceleration. *Phys. Plasmas* **2014**, *21*, 123113. [CrossRef]
22. Heigoldt, M.; Popp, A.; Khrennikov, K.; Wenz, J.; Chou, S.W.; Karsch, S.; Bajlekov, S.I.; Hooker, S.M.; Schmidt, B. Temporal evolution of longitudinal bunch profile in a laser wakefield accelerator. *Phys. Rev. ST Accel. Beams* **2015**, *18*, 121302. [CrossRef]
23. Guillaume, E.; Döpp, A.; Thaury, C.; Lifschitz, A.; Goddet, J.P.; Tafzi, A.; Sylla, F.; Iaquanello, G.; Lefrou, T.; Rousseau, P.; et al. Physics of fully-loaded laser-plasma accelerators. *Phys. Rev. ST Accel. Beams* **2015**, *18*, 061301. [CrossRef]
24. Wu, Y.; Yu, C.; Qin, Z.; Wang, W.; Zhang, Z.; Qi, R.; Feng, K.; Ke, L.; Chen, Y.; Wang, C.; et al. Energy Enhancement and Energy Spread Compression of Electron Beams in a Hybrid Laser-Plasma Wakefield Accelerator. *Appl. Sci.* **2019**, *9*, 2561. [CrossRef]
25. Katsouleas, T.; Wilks, S.; Chen, P.; Dawson, J.; Su, J. Beam loading in Plasma Accelerators. *Part. Accel.* **1987**, *22*, 81–99.
26. Rechatin, C.; Davoine, X.; Lifschitz, A.; Ismail, A.B.; Lim, J.; Lefebvre, E.; Faure, J.; Malka, V. Observation of Beam Loading in a Laser-Plasma Accelerator. *Phys. Rev. Lett.* **2009**, *103*, 194804. [CrossRef] [PubMed]

27. Ke, L.T.; Feng, K.; Wang, W.T.; Qin, Z.Y.; Yu, C.H.; Wu, Y.; Chen, Y.; Qi, R.; Zhang, Z.J.; Xu, Y.; et al. Near-GeV Electron Beams at a Few Per-Mille Level from a Laser Wakefield Accelerator via Density-Tailored Plasma. *Phys. Rev. Lett.* **2021**, *126*, 214801. [CrossRef]

28. Wang, W.; Feng, K.; Ke, L.; Yu, C.; Xu, Y.; Qi, R.; Chen, Y.; Qin, Z.; Zhang, Z.; Fang, M.; et al. Free-electron lasing at 27 nanometres based on a laser wakefield accelerator. *Nature* **2021**, *595*, 516–520. [CrossRef]

29. RadiaBeam: Plasma Photocathode Beam Brightness Transformer for Laser-Plasma-Wakefield Accelerators, DOE DESC0009533, 2013–2016. Available online: https://radiabeam.com/ (accessed on 17 December 2022).

30. Deng, A.; Karger, O.; Heinemann, T.; Knetsch, A.; Scherkl, P.; Manahan, G.; Beaton, A.; Ullmann, D.; Wittig, G.; Habib, A.; et al. Generation and acceleration of electron bunches from a plasma photocathode. *Nat. Phys.* **2019**, *15*, 1156–1160. [CrossRef]

31. Hidding, B.; Pretzler, G.; Rosenzweig, J.B.; Königstein, T.; Schiller, D.; Bruhwiler, D.L. Ultracold Electron Bunch Generation via Plasma Photocathode Emission and Acceleration in a Beam-Driven Plasma Blowout. *Phys. Rev. Lett.* **2012**, *108*, 035001. [CrossRef]

32. Chen, P. A possible final focusing mechanism for linear colliders. *Part. Accel.* **1987**, *20*, 171–182.

33. Bennett, W.H. Magnetically Self-Focussing Streams. *Phys. Rev.* **1934**, *45*, 890–897. [CrossRef]

34. Kuschel, S.; Hollatz, D.; Heinemann, T.; Karger, O.; Schwab, M.B.; Ullmann, D.; Knetsch, A.; Seidel, A.; Rödel, C.; Yeung, M.; et al. Demonstration of passive plasma lensing of a laser wakefield accelerated electron bunch. *Phys. Rev. Accel. Beams* **2016**, *19*, 071301. [CrossRef]

35. Thaury, C.; Guillaume, E.; Döpp, A.; Lehe, R.; Lifschitz, A.; Ta Phuoc, K.; Gautier, J.; Goddet, J.P.; Tafzi, A.; Flacco, A.; et al. Demonstration of relativistic electron beam focusing by a laser-plasma lens. *Nat. Commun.* **2015**, *6*, 6860. [CrossRef]

36. Chou, S.; Xu, J.; Khrennikov, K.; Cardenas, D.E.; Wenz, J.; Heigoldt, M.; Hofmann, L.; Veisz, L.; Karsch, S. Collective Deceleration of Laser-Driven Electron Bunches. *Phys. Rev. Lett.* **2016**, *117*, 144801. [CrossRef] [PubMed]

37. Eupraxia: European Plasma Research Accelerator with Excellence in Applications. 2015. Available online: https://roadmap2021.esfri.eu/projects-and-landmarks/browse-the-catalogue/eupraxia/ (accessed on 17 December 2022).

38. Sävert, A.; Mangles, S.P.D.; Schnell, M.; Siminos, E.; Cole, J.M.; Leier, M.; Reuter, M.; Schwab, M.B.; Möller, M.; Poder, K.; et al. Direct Observation of the Injection Dynamics of a Laser Wakefield Accelerator Using Few-Femtosecond Shadowgraphy. *Phys. Rev. Lett.* **2015**, *115*, 055002. [CrossRef]

39. D'Arcy, R.; Chappell, J.; Beinortaite, J.; Diederichs, S.; Boyle, G.; Foster, B.; Garland, M.J.; Caminal, P.G.; Lindstrøm, C.A.; Loisch, G.; et al. Recovery time of a plasma-wakefield accelerator. *Nature* **2022**, *603*, 58–62. [CrossRef]

40. Zgadzaj, R.; Li, Z.; Downer, M.; Sosedkin, A.; Khudyakov, V.; Lotov, K.; Silva, T.; Vieira, J.; Allen, J.; Gessner, S.; et al. Dissipation of electron-beam-driven plasma wakes. *arXiv* **2020**, arXiv:2001.09401.

41. Scherkl, P.; Knetsch, A.; Heinemann, T.; Sutherland, A.; Habib, A.F.; Karger, O.S.; Ullmann, D.; Beaton, A.; Manahan, G.G.; Xi, Y.; et al. Plasma photonic spatiotemporal synchronization of relativistic electron and laser beams. *Phys. Rev. Accel. Beams* **2022**, *25*, 052803. [CrossRef]

42. Steinke, S.; van Tilborg, J.; Benedetti, C.; Geddes, C.G.R.; Schroeder, C.B.; Daniels, J.; Swanson, K.K.; Gonsalves, A.J.; Nakamura, K.; Matlis, N.H.; et al. Multistage coupling of independent laser-plasma accelerators. *Nature* **2016**, *530*, 190–193. [CrossRef]

43. Raj, G.; Kononenko, O.; Gilljohann, M.F.; Doche, A.; Davoine, X.; Caizergues, C.; Chang, Y.Y.; Couperus Cabadağ, J.P.; Debus, A.; Ding, H.; et al. Probing ultrafast magnetic-field generation by current filamentation instability in femtosecond relativistic laser-matter interactions. *Phys. Rev. Res.* **2020**, *2*, 023123. [CrossRef]

44. Chen, M.; Sheng, Z.M.; Ma, Y.Y.; Zhang, J. Electron injection and trapping in a laser wakefield by field ionization to high-charge states of gases. *J. Appl. Phys.* **2006**, *99*, 056109. [CrossRef]

45. Zeng, M.; Chen, M.; Sheng, Z.M.; Mori, W.B.; Zhang, J. Self-truncated ionization injection and consequent monoenergetic electron bunches in laser wakefield acceleration. *Phys. Plasmas* **2014**, *21*, 030701.

46. Couperus, J.; Pausch, R.; Köhler, A.; Zarini, O.; Krämer, J.; Garten, M.; Huebl, A.; Gebhardt, R.; Helbig, U.; Bock, S.; et al. Demonstration of a beam loaded nanocoulomb-class laser wakefield accelerator. *Nat. Commun.* **2017**, *8*, 487. [CrossRef]

47. Manahan, G.; Habib, A.; Scherkl, P.; Delinikolas, P.; Beaton, A.; Knetsch, A.; Karger, O.; Wittig, G.; Heinemann, T.; Sheng, Z.; et al. Single-stage plasma-based correlated energy spread compensation for ultrahigh 6D brightness electron beams. *Nat. Commun.* **2017**, *8*, 15705. [CrossRef]

48. Kurz, T.; Heinemann, T.; Gilljohann, M.F.; Chang, Y.Y.; Couperus Cabadağ, J.P.; Debus, A.; Kononenko, O.; Pausch, R.; Schöbel, S.; Assmann, R.W.; et al. Demonstration of a compact plasma accelerator powered by laser-accelerated electron beams. *Nat. Commun.* **2021**, *12*, 2895. [CrossRef]

49. Corde, S.; Adli, E.; Allen, J.M.; An, W.; Clarke, C.I.; Clausse, B.; Clayton, C.E.; Delahaye, J.P.; Frederico, J.; Gessner, S.; et al. High-field plasma acceleration in a high-ionization-potential gas. *Nat. Commun.* **2016**, *7*, 11898. [CrossRef]

50. Couperus Cabadağ, J.P.; Pausch, R.; Schöbel, S.; Bussmann, M.; Chang, Y.Y.; Corde, S.; Debus, A.; Ding, H.; Döpp, A.; Foerster, F.M.; et al. Gas-dynamic density downramp injection in a beam-driven plasma wakefield accelerator. *Phys. Rev. Res.* **2021**, *3*, L042005. [CrossRef]

51. Schöbel, S.; Pausch, R.; Chang, Y.Y.; Corde, S.; Cabadağ, J.C.; Debus, A.; Ding, H.; Döpp, A.; Foerster, F.M.; Gilljohann, M.; et al. Effect of driver charge on wakefield characteristics in a plasma accelerator probed by femtosecond shadowgraphy. *New J. Phys.* **2022**, *24*, 083034. [CrossRef]

52. Foerster, F.M.; Döpp, A.; Haberstroh, F.; Grafenstein, K.v.; Campbell, D.; Chang, Y.Y.; Corde, S.; Couperus Cabadağ, J.P.; Debus, A.; Gilljohann, M.F.; et al. Stable and High-Quality Electron Beams from Staged Laser and Plasma Wakefield Accelerators. *Phys. Rev. X* **2022**, *12*, 041016. [CrossRef]

53. Ullmann, D.; Scherkl, P.; Knetsch, A.; Heinemann, T.; Sutherland, A.; Habib, A.F.; Karger, O.S.; Beaton, A.; Manahan, G.G.; Deng, A.; et al. All-optical density downramp injection in electron-driven plasma wakefield accelerators. *arXiv* **2020**, arXiv:2007.12634.

54. Knetsch, A.; Sheeran, B.; Boulton, L.; Niknejadi, P.; Põder, K.; Schaper, L.; Zeng, M.; Bohlen, S.; Boyle, G.; Brümmer, T.; et al. Stable witness-beam formation in a beam-driven plasma cathode. *Phys. Rev. Accel. Beams* **2021**, *24*, 101302. [CrossRef]

55. Habib, A.F.; Scherkl, P.; Manahan, G.G.; Heinemann, T.; Ullmann, D.; Sutherland, A.; Knetsch, A.; Litos, M.; Hogan, M.; Rosenzweig, J.; et al. Plasma accelerator-based ultrabright X-ray beams from ultrabright electron beams. In *Proceedings of the Advances in Laboratory-Based X-ray Sources, Optics, and Applications VII, San Diego, CA, USA, 13 August 2019*; International Society for Optics and Photonics: Bellingham, WA, USA, 2019; Volume 11110, p. 111100A.

56. Emma, C.; Van Tilborg, J.; Assmann, R.; Barber, S.; Cianchi, A.; Corde, S.; Couprie, M.E.; D'Arcy, R.; Ferrario, M.; Habib, A.F.; et al. Free electron lasers driven by plasma accelerators: Status and near-term prospects. *High Power Laser Sci. Eng.* **2021**, *9*, e57. [CrossRef]

57. Ferri, J.; Corde, S.; Döpp, A.; Lifschitz, A.; Doche, A.; Thaury, C.; Ta Phuoc, K.; Mahieu, B.; Andriyash, I.A.; Malka, V.; et al. High-Brilliance Betatron γ-Ray Source Powered by Laser-Accelerated Electrons. *Phys. Rev. Lett.* **2018**, *120*, 254802. [CrossRef]

58. Pompili, R.; Alesini, D.; Anania, M.P.; Arjmand, S.; Behtouei, M.; Bellaveglia, M.; Biagioni, A.; Buonomo, B.; Cardelli, F.; Carpanese, M.; et al. Free-electron lasing with compact beam-driven plasma wakefield accelerator. *Nature* **2022**, *605*, 659–662. [CrossRef]

59. Labat, M.; Cabadağ, J.C.; Ghaith, A.; Irman, A.; Berlioux, A.; Berteaud, P.; Blache, F.; Bock, S.; Bouvet, F.; Briquez, F.; et al. Seeded free-electron laser driven by a compact laser plasma accelerator. *Nat. Photonics* **2022**, 1–7. [CrossRef]

60. Habib, A.F.; Manahan, G.; Scherkl, P.; Heinemann, T.; Sutherland, A.; Altuiri, R.; Alotaibi, B.M.; Litos, M.; Cary, J.; Raubenheimer, T.; et al. Attosecond-Angstrom free-electron-laser towards the cold beam limit. *arXiv* **2022**, arXiv:2212.04398.